Z. Phys. B 101, 561–564 (1996)

ZEITSCHRIFT
FÜR PHYSIK B


# Global ac susceptibility of low pinning high-$T_c$ crystals near $T_c$

**M. Wurlitzer[1], F. Mrowka[1], P. Esquinazi[1], K. Rogacki[2,*], B. Dabrowski[2], E. Zeldov[3], T. Tamegai[4], S. Ooi[4]**

[1] Department Supercon. a. Magn., Universität Leipzig, Linnéstrasse 5, D-04103 Leipzig, Germany
[2] Department of Physics and The Science and Technology Center for Superconductivity, Northern Illinois University, De Kalb, IL 60115, USA
[3] Department of Condensed Matter Physics, The Weizmann Institute of Science, 76100 Rehovot, Israel
[4] Department of Applied Physics, The University of Tokyo, Hongo, Bunkyo-ku, Tokyo 113, Japan

Received: 7 March 1996 / Revised version: 7 May 1996

**Abstract.** We have studied the hysteretic loss and the shielding capability of $Bi_2Sr_2CaCu_2O_8$ and $YBa_2Cu_4O_8$ crystals as a function of ac field ($\mu_0 H \leq 1$mT), frequency, and temperature at small dc fields ($\mu_0 H_a < 1$ mT) near the critical temperature $T_c$. We show that the global ac field dependence of the susceptibility can be described in terms of a geometrical barrier model in agreement with local permeability results. At temperatures very near $T_c$, however, we observe a crossover to diffusive behavior. The frequency dependence of the temperature of the dissipation maximum at finite dc fields shows a thermally activated behavior.

**PACS:** 74.60.Ge;74.72.Bk;74.72.Hs

Recently published measurements of the local permeability in clean $Bi_2Sr_2CaCu_2O_8$ crystals near the critical temperature $T_c$ and at low enough dc fields ($\mu_0 H_a \leq 10$ mT) in perpendicular geometry have shown that the ac response of the superconductor can be interpreted in terms of a potential barrier of geometrical origin [1] This geometrical barrier is related to the rectangular (or in general non-elliptic) cross section of a flat sample in transverse fields which influences the flux line energy distribution. If pinning is negligible and if the applied transverse field is non zero, a vortex is driven towards the center of the sample by the Lorenz force of the Meissner current. The vortex energy is then given by two terms: (a) line energy $\times$ vortex length ( = thickness $d$ of a rectangular sample) and (b) the integral of the Lorenz force. The exact analytical solution for the current and field distribution in this case indicates that the vortex energy has a minimum only at the center of the sample and close to the edges is positive and very large [1]. This interesting result is in clear contrast with the behavior observed at lower temperatures and at larger dc fields where the ac response can be interpreted in terms of bulk pinning properties through the diffusion constant (or electrical resistivity) [2].

In this work we have studied the ac field, frequency, and temperature dependence of the global ac susceptibility of low pinning high-$T_c$ crystals near $T_c$ and at dc fields $\mu_0 H_a \leq 1$ mT in perpendicular geometry. Our aim is to investigate to what extent the global ac response of the crystals can be interpreted in terms of a geometrical barrier and if thermally activated processes at low dc fields and near $T_c$ are important in low pinning high-$T_c$ crystals. We note that the influence of thermally activated processes to the ac response of high-$T_c$ superconductors were unambiguously proved in the past by different experimental methods, but at relatively large dc fields. One purpose of our work is to extend this investigation to lower dc fields.

High quality $YBa_2Cu_4O_8$ (Y124) crystals were grown using the self-flux method at a high oxygen pressure of 600 bar at 1100°C [3]. Crystal uniformity and chemical composition were examined using a Hitachi S-2700 Scanning Electron Microscope with an Oxford Link microprobe. The critical temperature of the crystal investigated in this work at zero dc field and at ac field $\mu_0 H_0 \sim 1$ μT was $T_c = 78.5$ K. The crystal geometry was: length $l = 600$ μm, width $w = 440$ μm, and thickness $d = 20$ μm. The critical current of the crystals (calculated from the magnetization loops taken at different temperatures below 70 K) was $j_c \simeq 4 \times 10^5$ A/cm$^2$ at 6 T and 5 K and decreased by four times at 20 K. From ac susceptibility measurements at 77 K and at zero dc field we estimate $j_c \simeq 10^3$ A/cm$^2$.

The $Bi_2Sr_2CaCu_2O_8$ (Bi2212) crystal studied in this work was prepared by traveling solvent floating zone technique. The crystal showed a transition temperature $T_c = 88.0$ K. The geometry of the crystal was $l = 1100$ μm, $w = 900$ μm and $d = 30$ μm. The susceptibility measurements were performed with a Lake Shore 7000 AC Susceptometer. The susceptometer is designed for operation at low level ac magnetic fields $\mu_0 H \leq 1$ mT and dc fields $\mu_0 H_a \leq 1$ mT. The earth magnetic field ( = 0.035 mT) was

* On leave from Institute of Low Temperature and Structure Research, Polish Academy of Sciences, PL-50-950 Wroclaw, Poland

not shielded. The temperature stability of the susceptometer was 0.05 K at 80 K. The ac field dependence of $\chi$ was measured sweeping the ac field at constant temperature; the frequency dependence was measured sweeping the temperature at constant ac field ten times smaller than the applied dc field.

A theoretical description of the hysteretic magnetization and the local ac response in presence of a geometrical barrier has been published in [1,4,5]. We describe below the necessary steps for the calculation of the global ac susceptibility in presence of geometrical barriers. We consider a thin superconducting strip of rectangular cross section of width $w = 2W(-W \le x \le W)$, and thickness $d(-d/2 \le z \le d/2 \ll W)$ which infinitely extends in the y direction. The applied ac field $H(t) = H_0 \sin(\omega t)$ (or the dc field $H_a$) is along the positive z direction, i.e. transverse geometry. We define the real $\chi'$ and imaginary $\chi''$ parts of the susceptibility as a function of the global magnetization $M$ as follows:

$$\chi' = \frac{2}{\pi H_0} \int_0^{\tau} M(H) \sin(\omega t)\, d(\omega t) \tag{1}$$

$$\chi'' = \frac{2}{\pi H_0} \int_0^{\tau} M(H) \cos(\omega t)\, d(\omega t) \tag{2}$$

Furthermore, we define the following reduced variables: $h(t) = H(t)/H_{c1}$ and $M_r = M/(H_{c1}/4\pi)$.

At fields $0 \le h \le h_p = (2/\pi) \operatorname{arctanh} \sqrt{1 - (1 - (d/2W))^2}$ vortices (depicted as shaded areas in Fig. 1 (upper part)) penetrate only at the edges $|x| \ge e = W - d/2$ and the magnetization is $M_r(h) = -(W/d)\tanh(\pi h/2)$ which corresponds to region A in Fig. 1 (lower part).

At fields $h_p < h \le h_m$, where $h_m$ is the maximum applied field, vortices overcome the potential barrier irreversibly and, in case of zero bulk pinning, the vortices penetrate to the center of the sample in a width $0 \le 2b \le 2b_m < 2e = 2(W - (d/2))$ driven by the Lorentz force of the Meissner currents, see Fig. 1, region B. The magnetization in this case is given by $M_r(h) = -(W/d)(1 - [1 - (d/2W)]^2)\coth(\pi h/2)$.

If we decrease the field $h$ within $h^* \le h \le h_m$ (region C in Fig. 1) the magnitude of the magnetization decreases. The half width $b$ and the distance $e$ vary in the region $b_m \le b \le b^*$ and $(W - d/2) \le e \le e^*$. The values of $b$ and $e$ are determined by the condition that the flux in the width $2b$ in the middle of the sample remains constant, i.e.

$$\int_{-b}^{+b} B(x)\, dx = \text{const}, \tag{3}$$

with the internal field $B(x)$ given by [4]

$$B(x) = \frac{2H_{c1}}{\pi} \ln \frac{\sqrt{|e^2 - x^2|(W^2 - b^2)} + \sqrt{|b^2 - x^2|(W^2 - e^2)}}{\sqrt{(e^2 - b^2)|W^2 - x^2|}}, \tag{4}$$

and the applied field by

$$h = \frac{2}{\pi} \ln \frac{\sqrt{W^2 - b^2} + \sqrt{W^2 - e^2}}{\sqrt{e^2 - b^2}}. \tag{5}$$

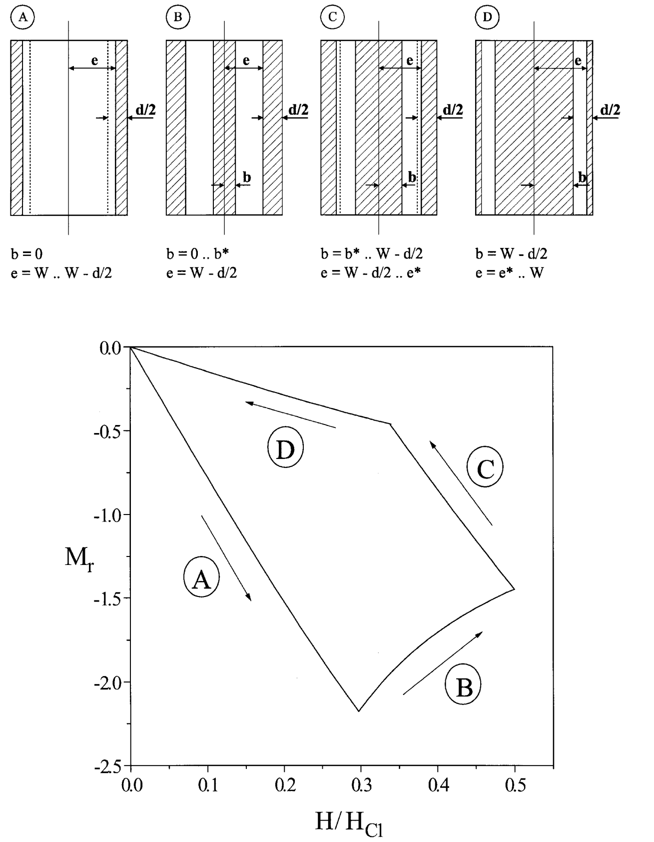


**Fig. 1.** Upper part: Shaded areas indicate the regions where flux lines are present at different applied fields. $2W$ is the width of the sample and the magnetic field is applied perpendicular the plane of the paper. Lower part: calculated magnetization loop as a function of the reduced applied field $h = H/H_{c1}$ for the special case $W/d$ (half width/thickness) = 0.2, $h_m = 0.5$

The magnetization can be calculated using

$$M_r = -\frac{1}{Wd}\sqrt{(W^2 - b^2)(W^2 - e^2)} \tag{6}$$

after obtaining numerically the functions $b(h)$ and $e(h)$. The results of the calculation, region C in Fig. 1, indicate that the magnitude of the magnetization decreases nearly linearly with decreasing the applied field $h$.

For $0 \le h \le h^*$ the vortices leave the sample at the edges; the width $b = W - d/2$ and the distance $e$ varies between $W - d/2 \le e^* \le W$. The height of the dome (Eq. (4)) decreases. The magnetization is $M_r(h) = (-W/d)(1 - [1 - (d/2W)]^2)\tanh(\pi h/2)$, see Fig. 1, region D.

With the complete magnetization curve in a field cycle we can calculate both parts of the susceptibility. The results obtained for two different ratios $W/d$ are shown in Fig. 2. As expected the critical penetration field $h_p$ increases with the thickness of the sample. It is also interesting to note that the maximum of the imaginary part of the susceptibility is not constant – as for example in the case of bulk pinning non-linear Bean model ($\simeq 0.24$ [6] or TAFF ($\simeq 0.42$) – but depends on the ratio $W/d$.

Figure 3 shows the susceptibility for the Y124 single crystal as a function of the reduced field $H_0/H_{\max}$ at different constant temperatures. $H_{max}$ denotes the ac field at the dissipation maximum. The theory fits very well the experimental data. Note that in the normalized coordinates of Fig. 3 the theoretical curve is calculated without free parameters since the ratio $W/d$ is measured. The inset in Fig. 3 shows the lower critical field $H_{c1}(T)$ obtained from the comparison with theory, i.e. at the reduced field $h_p$ where the dissipation increases abruptly. For the highest measured temperature 78.3 K in this crystal we observe clear deviations from the geometrical barrier model, see Fig. 3. Strikingly the ac field dependence of the susceptibility resembles the dependence obtained from the non-linear Bean model after Brandt [6]. The same feature is observed in the Bi2212 crystal.

Figure 4 shows the two components of the ac susceptibility as a function of the reduced ac field for the Bi2212 crystal. The geometrical barrier model fits well the observed ac field dependence and absolute values of the susceptibility at reduced temperatures $t \leq 0.94$. At higher temperatures, however, we observe similar deviations as in the Y124 crystal: the value of $\chi''$ at the maximum decreases and there is a broadening of the ac field dependence which tends to the curve obtained from the non-linear Bean model for transverse geometry [6].

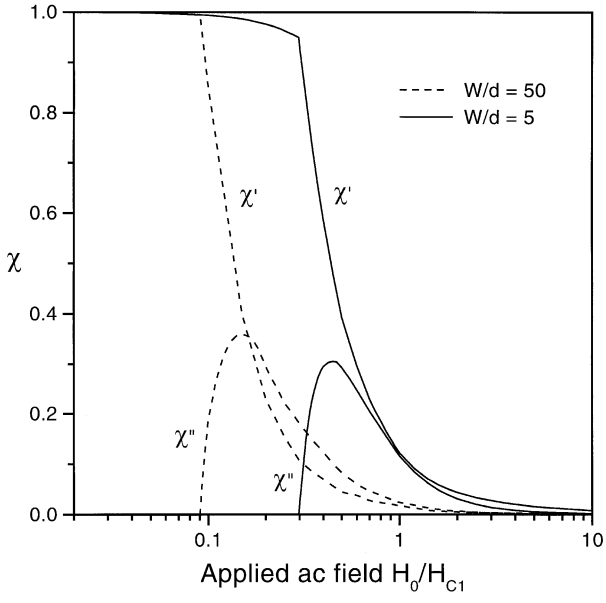


**Fig. 2.** Real and imaginary parts of the normalized susceptibility as a function of the amplitude of the ac field for two different ratios $W/d$ according to the geometrical barrier model

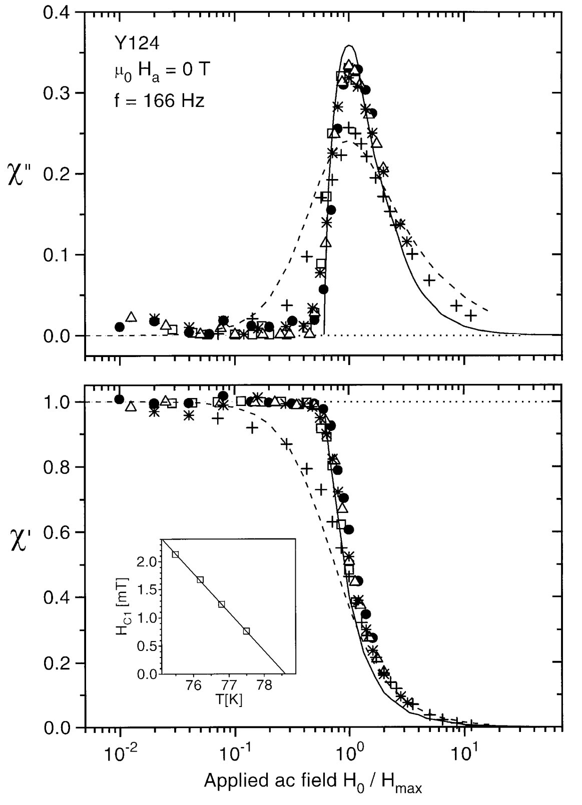


**Fig. 3.** Real and imaginary parts of the normalized susceptibility as a function of the amplitude of the ac field for the Y124 crystal at different temperatures: 75.5 K (□), 76.2 K (●), 76.8 K (△), 77.5 K (✱), 78.3 K ( + ). The corresponding values of $H_{max}$ are: 0.88 mT, 0.63 mT, 0.5 mT, 0.31 mT and 0.09 mT respectively. The continuous line was calculated with the geometrical barrier model and the dashed line follows the non-linear Bean model for a strip after Brandt [6]. Inset: Lower critical field $H_{c1}$ as a function of temperature

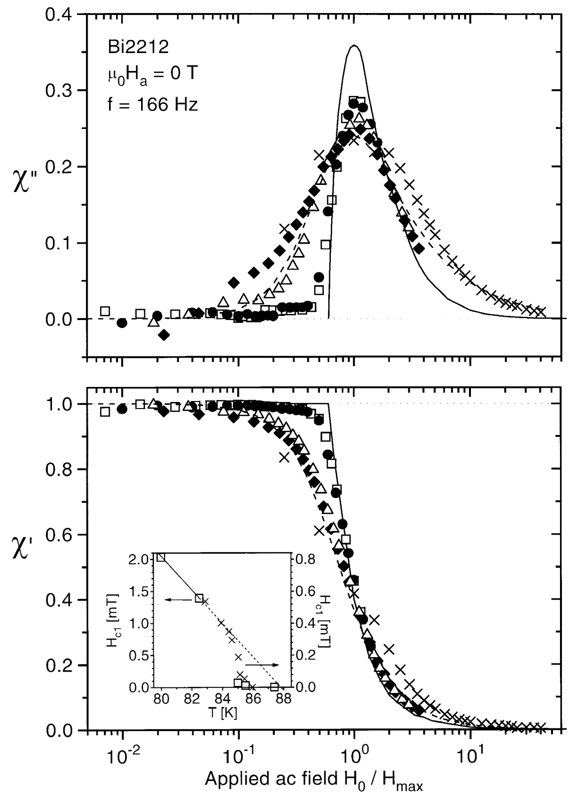


**Fig. 4.** Real and imaginary parts of the susceptibility as a function of ac field for the Bi2212 crystal at different temperatures: 80.0 K (□), 82.5 K (●), 85.0 K (△), 85.5 K (◇), 87.4 K ( × ). The corresponding values of $H_{max}$ are: 0.88 mT, 0.63 mT, 0.34 mT, 0.28 mT and 0.03 mT respectively. The continuous line was calculated with the geometrical barrier model and the dashed line follows the non-linear Bean model for a strip [6] Lower critical field $H_{c1}$ as a function of temperature: this work (□) and as taken from [7] (the temperature scale was normalized to take into account the different $T_c$)

Note that in the case of TAFF $\chi''_{\max} \simeq 0.42$. Similar results have been obtained for another crystal taken from a different batch.

The ac field dependence of the global susceptibility in both crystals and at *no applied dc field* (excluding the earth field) indicates that at temperatures very near the critical one there is a crossover in the main mechanism of hysteretic behavior, i.e. from geometrical barrier to bulk effects. This result appears to be in contradiction with the expectations that only geometrical barrier should be active near $T_c$ [1]. The apparent easy vortex penetration might be due to structural and/or compositional irregularities in the crystal with reduced $T_c$ and therefore smaller geometrical barriers. In addition we should take into account that the geometrical barrier decreases with temperature and vanishes at $T_c$ since it is proportional to $H_{c1}(T)$. In [7] a strong suppression of the first penetration field $H_p$ in Bi2212 crystal has been observed very near $T_c$. The suppression of $H_p$ has been tentatively interpreted as due to the two dimensional character of the Bi2212 crystal and the appearance of thermally induced vortex-anti-vortex pairs just below $T_c$ [8]. The suppression of $H_{c1}$ has been also observed in Y123 crystals [9]. In the inset of Fig. 4 we have plotted the calculated values of $H_{c1}(T)$. The temperature region where we observed the broadening of the ac susceptibility response agrees well with the temperature region where $H_{c1}$ is suppressed. Due to the smaller anisotropy of the Y124 crystal the suppression of $H_{c1}$ should be closer to $T_c$ compared to Bi2212 in agreement with our results, see Fig. 3.

The geometrical barrier model does not include any frequency dependence for the ac susceptibility. This is not in agreement with our experimental observations at small applied dc fields. Figure 5 shows the frequency of the ac field for both crystals as a function of the reciprocal of the temperature $T_{\max}$ where $\chi''$ shows a maximum, measured at applied dc fields of 1 mT, 0.3 mT and 0 T (for Bi2212 only). At 1 mT and in the frequency range of the measurements we observe a typical Arrhenius behavior. From the plots we obtain the following effective activation energies for Y124 (Bi2212): $\sim 6$ eV ($\sim 3$ eV). These values are in reasonable agreement with extrapolated data from literature obtained from, for example, the resistivity transition in an applied magnetic field [10]. These activation energies are at least one order of magnitude smaller than the maximum geometrical energy barrier $H_{c1}\phi_0 d/4\pi$ with $H_{c1}(t \sim 0.98) \sim 1$ mT for the Y124 crystal. Measurements at dc fields of $\sim$ 0.5 mT and ac field of 0.1 mT of a second crystal from the same crucible show a shift of 0.15 K in the maximum of $\chi''$ by changing the frequency from 200 Hz to 5 kHz.

Since from the ac field dependence of the susceptibility at *no applied dc field* and at low enough temperatures no clear evidence for thermal activation is observed (see Figs. 3 and 4), we expect that the effective activation energy increases at fields smaller than 1 mT. This is indeed observed in the Bi2212 crystal where the frequency dependence of the dissipation has been measured at 0.3 mT and 0 T dc field, see Fig. 5. It remains to be clarified in future experiments how the geometrical barrier and bulk pinning (with and without thermally activated processes) influence the ac field dependence of the susceptibility at non zero dc fields.

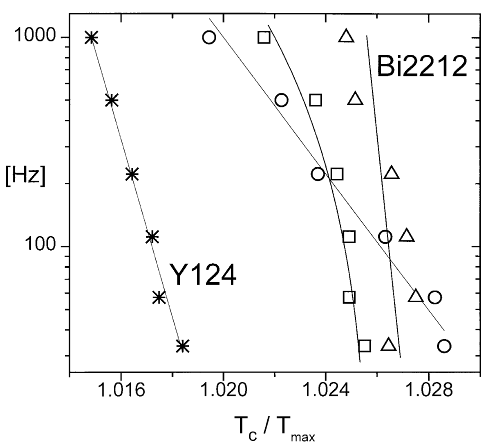


**Fig. 5.** Logarithm of the frequency of the ac field as a function of $T_c/T_{\max}$ ($T_{\max}$ is the temperature of the dissipation maximum) for the Y124 and Bi2212 crystals at dc fields of 1 mT ($*$, $\circ$) and, for Bi2212 only, 0.3 mT ($\square$) and 0 T ($\triangle$, ac field amplitude 0.03 mT). Lines are only a guide to the eye

We conclude that the ac field dependence of the global ac susceptibility of low pinning high-$T_c$ crystals at low dc fields can be interpreted in terms of geometrical barrier model in agreement with local susceptibility results. At temperatures very near $T_c$ our results indicate that the effective geometrical barrier becomes smaller (or vanishes) than the bulk pinning. This may be caused by suppression of $H_{c1}$ very near $T_c$ as observed in [7, 9]. The frequency dependence of the dissipation maximum at finite dc fields indicates thermally activated behaviour.

We wish to acknowledge fruitful discussions with E.H. Brandt. This work is supported by the German-Israeli Foundation for Scientific Research and Development – GIF under Grant G-303-114.07/93. The work at NIU is supported by the National Science Foundation under Grant DMR 91-20000.3, and the work at Tokyo University by Grant-in-Aid for Scientific Research from the Ministry of Education, Science and Culture, Japan.

## References

1. Morozov, N., Zeldov, E., Majer, D., Khaykovich, B.: Phys, Rev. Lett. **76**, 138 (1996)
2. See for example the review on vibrating reed measurements: Ziese, M., Esquinazi, P., Braun, H.F.: Supercond. Sci. Technol. **7**, 869 (1994)
3. Dabrowski, B., Zhang, K., Pluth, J.J., Wagner J.L., Hinks, D.G.: Physica C **202**, 271 (1992)
4. Zeldov, E. et al.: Phys. Rev. Lett. **73**, 1428 (1994)
5. Benkraouda, M., Clem, J.R.: (preprint)
6. Brandt, E.H., Indenbom, M., Forkl, A.: Europhys. Lett. **22**, 735 (1993); Phys. Rev. B **49**, 9024 (1994); idem **50**, 4034 (1994); idem **50**, 13833 (1994)
7. Brawner, D.A. et al.: Phys. Rev. Lett. **71**, 785 (1993)
8. Bulaevskii, L.N., Ledvij, M., Kogan, V.G.: Phys. Rev. Lett. **68**, 3773 (1992)
9. Safar, H. et al.: In Progress in High Temperature Superconductivity, Vol. 25, p. 140. Nicolvsky R. (ed.) Singapore: World Scientific, 1990, Pastoriza, H. et al., Physica B **194–196**, 2237 (1994)
10. For Y124 see, for example, Krelaus J. et al.: In: Applied Superconductivity, p. 783 Freyhardt, H. (ed.) DGM, Germany 1993